

Article

Mechanical Properties of a Bio-Composite Produced from Two Biomaterials: Polylactic Acid and Brown Eggshell Waste Fillers

Duncan Cree ^{1,*} , Stephen Owuamanam ¹ and Majid Soleimani ²

¹ Department of Mechanical Engineering, University of Saskatchewan, Saskatoon, SK S7N 5A9, Canada; stephen.owuamanam@usask.ca

² Department of Chemical and Biological Engineering, University of Saskatchewan, Saskatoon, SK S7N 5A9, Canada; mas233@mail.usask.ca

* Correspondence: duncan.cree@usask.ca; Tel.: +1-306-966-3244

Abstract: An option to reduce the exploitation and depletion of natural mineral resources is to repurpose current waste materials. Fillers are often added to polymers to improve the properties and lower the overall cost of the final product. Very few studies have assessed the use of waste brown eggshell powder (BESP) as filler in polylactic acid (PLA). The addition of mineral fillers in a polymer matrix can play an important role in the performance of a composite under load. Therefore, tailoring the amount of filler content can be a deciding factor as to which filler amount is best. The goal of this study was to investigate the effect of brown eggshells compared to conventional limestone (LS) powder on the mechanical properties of PLA composites. One-way analysis of variance (ANOVA) was used to carry out the statistical analysis on the average values of each composite mechanical property tested. Scanning electron microscopy (SEM) was used to view if there were any differences in the fractured surfaces. Overall, the LS performed marginally better than the BESP fillers. The highest ultimate tensile and ultimate flexural strengths for eggshell composites containing 32 μm fillers had values of 48 MPa (5–10 wt.% BESP) and 67 MPa (10 wt.% BESP), respectively. Both the tensile and flexural modulus improved with filler contents and were highest at 20 wt.% with values of 4.5 GPa and 3.4 GPa, respectively. The Charpy impact strength decreased for all filler amounts. SEM micrographs identified changes in the fractured surfaces due to the additions of the filler materials. The ANOVA results showed statistically significant differences for the composite materials. After five weeks of soaking in distilled water, the composites containing 20 wt.% BESP fillers had the highest weight gain. The study demonstrated that waste brown eggshells in powdered form can be used as a filler in PLA composites.

Keywords: conventional limestone; waste brown eggshells; polylactic acid; mechanical properties; bio-composite



Citation: Cree, D.; Owuamanam, S.; Soleimani, M. Mechanical Properties of a Bio-Composite Produced from Two Biomaterials: Polylactic Acid and Brown Eggshell Waste Fillers. *Waste* **2023**, *1*, 740–760. <https://doi.org/10.3390/waste1030044>

Academic Editors: Catherine N. Mulligan, Vassilis Athanasiadis and Dimitris P. Makris

Received: 21 July 2023

Revised: 11 August 2023

Accepted: 22 August 2023

Published: 1 September 2023



Copyright: © 2023 by the authors. Licensee MDPI, Basel, Switzerland. This article is an open access article distributed under the terms and conditions of the Creative Commons Attribution (CC BY) license (<https://creativecommons.org/licenses/by/4.0/>).

1. Introduction

Polymers are used in many applications where synthetic thermoplastics are the most-popular and account for nearly 80% of all plastics around the world [1]. After their lifespan, developed countries tend to recycle them somewhat more than under-developed countries, where plastics are discarded to landfills. From 1950 to 2015, it is estimated that 6.3 billion metric tonnes (BMT) of plastic waste have been produced globally and about 60% or 4.9 BMT have been accumulating in landfills or the environment. If this waste trend continues, the amount of plastics discarded will reach an estimated 12 BMT by 2050 [2]. Recently, micro- and meso-plastics have been a growing problem in the marine environment [3]. According to Lebreton et al. [4], the Great Pacific Garbage Patch, a region in the North Pacific Ocean, has accumulated floating plastics in an area estimated to be 1.6 million km^2 [4]. Putting this into perspective, it is about 2.5-times the size of France (based on its land area of 643,801 km^2). Plastic degradation in the environment can take a

long time. For example, depending on the type of plastic, it is estimated that plastic bottles can take 70–450 years to decompose, while plastic bags can take 10–1000 years [5].

Polylactic acid (PLA) is a bio-plastic product made from fermented plants such as corn, wheat, and sugarcane, which is derived from renewable and sustainable biomass sources. In order to lower the carbon footprint, PLA can be an alternative to petroleum-based synthetic thermoplastics. PLA has the largest market segment of all bioplastics produced. In 2022, the PLA global production was 20.7% or 460,000 tonnes and is estimated to reach 37.9% or about 2,390,000 tonnes by 2027 [6]. Presently, packaging relies heavily on synthetic polymers. A shift to bio-plastics could reduce contamination from these plastic products into the environment through biodegradation. PLA can be biodegraded by traditional composting [7] or mechanical [8] and chemical [9] recycling. A study showed that PLA has the ability to fully degrade into non-toxic products in a composting facility under specific conditions of temperature (30–60 °C), humidity (30–70%), and pH (8.5) over a period of 28–98 days [7]. Mechanical recycling consists of cleaning, drying, cutting, and pelletizing before reprocessing into new materials [8]. Chemical recycling involves the breakdown of PLA using solvents without affecting the monomer structure [9].

Lower-cost fillers such as calcium carbonate are used in polymer materials generally to reduce the overall cost of the polymers. Among other properties, fillers improve the tensile modulus and toughness of polymers. For instance, Zuiderduin et al. (2003) [10] added 0 to 60 wt.% of calcium carbonate to polypropylene (PP). Although the tensile strength decreased with the increase in filler loading, the tensile modulus and impact toughness increased within the tested temperature range of 20–70 °C compared to pure PP. The authors highlighted that a good dispersion of particulates within the matrix was important as agglomeration tended to have detrimental effects on the properties. Similarly, synthetic polymers containing calcium carbonate powder as fillers have been studied for polypropylene (PP) [11], LDPE [12–15], and HDPE [16,17] thermoplastic matrices.

The brown eggshell waste used in this study was acquired from the poultry industry, where they are composed of 96–97 wt.% calcium carbonate, a common ingredient found in geological formations of mineral limestone, with organic membranes as the balance [18]. Although both white and brown eggs are available on the market, the calcium carbonate content in the shells were found to be comparable [19]. Collecting eggshells from homes and restaurants would be a difficult task; however, there are large amounts of eggshell waste being produced every day by an industrial breaking plant process, which produces liquid eggs in bulk. There are many breaking plants located throughout the world. For instance, Egg Processing Innovations Cooperative is an egg-breaking plant located in Canada, which can process 180,000 dozen eggs per week. Newly emerging companies around the globe such as Eco-SHELL in Spain, Ateknea Solutions Hungary LLC in Hungary, and Bionovel Plus DOO in the Republic of Macedonia are advancing technology for extracting calcium carbonate powders from eggshells. Within a short time, these companies will want to find new niches for their powdered eggshells. The use of white eggshell powders in new materials has been suggested as alternative fillers in polymers, paints, ceramic tiles, mortar, and concrete [18]. A number of studies have been conducted on the use of white eggshells and seashells (e.g., bio-limestone) in synthetic thermoplastic polymers. For example, the mechanical properties have been evaluated for polypropylene (PP)/eggshells [20–24], LDPE/eggshells [25,26], LDPE/oyster shell [27] and for polyester (PET)/eggshells [28].

The prospect of using a green PLA polymer inspires the use of a sustainable filler material. Very few studies have been conducted on calcium carbonate fillers derived from eggshells for use in PLA composites. Hassan et al. (2014) [29] studied the effect of adding white eggshell powders to a biodegradable Bioplast thermoplastic polymer. The results showed that adding 1–2 wt.% eggshell filler improved the flexural strength and modulus, possibly due to the evenly dispersed particles throughout the matrix. Ashok et al. (2014) [30] investigated the addition of white eggshell fillers in PLA films. At all levels, the tensile strength and modulus increased, where the highest improvements were with 4 wt.% filler additions. The authors observed that the particles were uniformly distributed when

less than 4 wt.% fillers were added, while at 5 wt.%, agglomeration occurred. More recently, Cree and Soleimani (2023) [31] investigated the addition of white eggshell powders to PLA. The tensile and flexural strengths peaked when 5 wt.% and 10 wt.% fillers were added, respectively, while the tensile and flexural modulus both improved as the filler loading increased. The dispersion of particles in a polymer matrix was noted to be difficult to achieve, which may affect the properties of the polymer composite materials.

In this work, calcium-carbonate-based filler; conventional limestone (LS), and brown eggshell powder (BESP) were added to a PLA matrix using an extrusion injection method. The brown chicken eggshells were initially crushed, washed, and dried prior to fine grinding, and both filler types were sieved to a particle size of 63 μm and 32 μm . The goal was to investigate the effect of adding various quantities of calcium carbonate powder to virgin PLA. The ultimate tensile, ultimate flexural, and impact toughness properties, fractured morphology, and water absorption, with and without calcium carbonate fillers, were studied. Statistical analysis of the mechanical property results was conducted using analysis of variance (ANOVA) to determine if a statistically significant difference existed between the average values of the composites containing filler loadings. After five weeks of soaking in distilled water, the moisture content and mass loss were measured. Water samples from each beaker were assessed for calcium carbonate contents and pH levels. The novelty of this study highlights the properties of PLA containing brown eggshells as a sustainable filler material.

2. Materials and Methods

2.1. Materials

The injection molding matrix was virgin PLA Prime Natural 4043D (NatureWork[®] LLC, Minnetonka, MN, USA) in pellet form. Conventional limestone was obtained from Imasco Minerals Inc. (Surrey, BC, Canada), while brown eggshells were obtained from Maple Lodge Hatcheries Ltd. (Stratford, ON, Canada).

2.2. Eggshell Preparation

The brown eggshells were dry-crushed in a steel drum, as shown in Figure 1a, which contained eleven 50.8 mm (2 in)-diameter steel balls (not visible). Prior to drying, the coarse eggshells were agitated and thoroughly washed several times to remove the organic membranes from the eggshells. A detailed explanation of the process can be obtained from a recent study [19]. To decrease the particle dimensions, a ball mill containing ceramic spheres was used, followed by rinsing with water and drying at 105 °C for 24 h. The ball mill jar with dimensions of 290 mm \times 550 mm (diameter \times length) is shown in Figure 1b and the pulverized brown eggshell powder (BESP) along with the ceramic balls ranging in diameter from 24–38 mm in Figure 1c. To evaluate the role of the filler particle size, the conventional limestone and eggshell powders were sieved to final mesh sizes of 230 (63 μm) and 450 (32 μm).

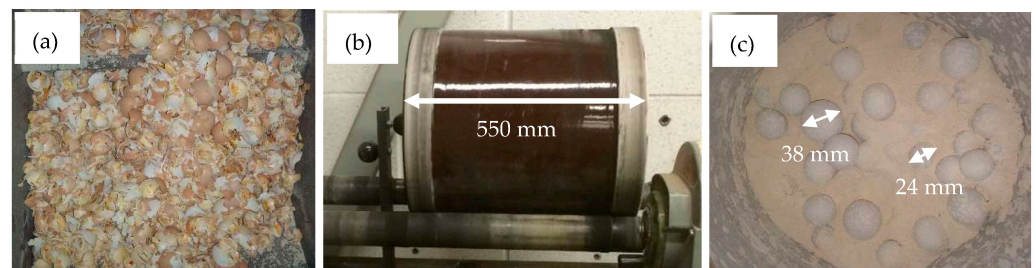


Figure 1. BESP preparation: (a) view inside steel drum, (b) ball mill, and (c) view inside ball mill.

2.3. Composite Formulations

A three-step process was used to fabricate the composite materials. First, the PLA pellets and calcium carbonate powders were mixed in a twin-screw extruder (SHJ-35, Nanjing Yougteng Chemical Equipment Co. Ltd., Nanjing, China). The extrusion was conducted at a temperature of 175 °C and a screw rotational speed of 16 rpm. Then, the filaments leaving the extruder were cooled in a water bath and further pelletized. The pellets were then dried at 80 °C for 4 h prior to injection molding. Finally, the composites were injection molded (Shen Zhou 2000, Zhangjiagang Shen Zhou Machinery Co., Shenzhen, China) with a temperature profile of 175, 180, 185, and 190 °C (feed zone to die zone). Compared to the virgin PLA (the control), the amount of filler loadings for each PLA composite formulation is shown in Table 1. The calcium carbonate fillers (LS and BESE) were used to replace a portion of the PLA polymer. The injection mold die was only able to produce tensile dog bone specimens and water absorption samples. The flexure and Charpy impact toughness specimens were made from the center of the dog bone samples cut to different lengths, but within ASTM standard sizes.

Table 1. PLA composites containing LS and BESE loadings for 63 µm and 32 µm particles.

Sample	Calcium Carbonate Contents		
	PLA (wt.%)	LS (wt.%)	BESE (wt.%)
Virgin PLA	100	0	0
LS-5	95	5	0
LS-10	90	10	0
LS-20	80	20	0
BESE-5	95	0	5
BESE-10	90	0	10
BESE-20	80	0	20

2.4. Mechanical Characterization

Tensile and flexural measurements were conducted using an Instron series 1137 (Instron, MA USA) instrument according to ASTM D638-14 and ASTM D790-17, respectively. The dimensions of the tensile specimens measured 200 mm × 12.74 mm × 3.25 mm, while the flexural specimens measured 65 mm × 12.74 mm × 3.25 mm (l × w × t). The tensile specimens were tested using a 10 kN load cell and a crosshead speed of 5 mm/min, while the three-point flexural test employed a 250 N load cell with a calculated crosshead speed of 1.30 mm/min. To retain a support span-to-depth ratio of 16:1, a 50 mm span length was used. For both tensile and flexural experiments, five specimens were tested for each composition at room temperature and averaged. Un-notched Charpy impact tests were conducted at room temperature using an Instron 450 MPX pendulum impact machine according to the guidance of ASTM D6110-18. The specimen's dimensions were 56 mm × 12.74 mm × 3.25 mm (l × w × t). At least ten samples were tested for each composite formulation and the mean values obtained. Prior to conducting the mechanical tests, all samples were conditioned at 23 ± 3 °C with a relative humidity of 50 ± 4% for about 24 h.

2.5. Scanning Electron Microscopy

The calcium carbonate particles and fractured surfaces of the tensile, flexure, and Charpy impact toughness samples were investigated using a JEOL JSM-6010 Scanning Electron Microscope (JEOL Ltd., Tokyo, Japan) in secondary electron (SEI) mode. All samples were initially gold coated to prevent electrostatic charging during viewing and observed at an operating voltage of 10–20 kV.

2.6. Water Uptake

The water uptake tests were conducted according to the recommended procedure outlined in ASTM D570-22. Test specimens measuring 57.4 mm × 36.4 mm × 2.7 mm (l × w × t) were performed at room temperature on a set of three samples placed in beakers filled with distilled water. Before beginning the experiments, all specimens were placed in an oven at 50 °C for 24 h. They were then removed, allowed to cool down in a desiccator, and weighed to obtain the initial dry weights. The weight gain percentage due to water absorption over a period of 5 weeks was initially measured after 24 h (1 day) followed by one-week intervals until saturation was reached using a digital balance (±0.1 mg). The specimens were removed one by one and quickly dried using a paper towel to remove excess surface water. The percentage of mass gain due to moisture uptake was measured by Equation (1), while the mass loss was evaluated by Equation (2).

$$\text{Moisture content (\%)} = [(m_2 - m_1)/m_1] \times 100\% \quad (1)$$

$$\text{Mass loss (\%)} = [(m_3 - m_1)/m_1] \times 100\% \quad (2)$$

where moisture content is the percentage mass gain, m_1 is the initial oven-dry mass, m_2 is the mass after every soaking interval, and m_3 is the mass after the 5-week period.

2.7. Leaching Measurements

To determine if calcium carbonate was coming out of the composite during the 5-week of water immersion, water samples from each uptake test were examined with an atomic absorption spectrophotometer (Model 240 Series AA, Agilent Technologies, Santa Clara, CA, USA).

2.8. pH Measurements

To determine if there were changes due to the degradation of the PLA and the leaching of the calcium carbonate fillers after a 5-week period in distilled water, the pH levels were measured with a pH meter (Orion StarTM A111 pH Benchtop Meter; Thermo Scientific Ward Hill, MA, USA) in triplicate. The distilled water was not refreshed during the 5-week period, where silicone caps were placed on the beakers to avoid evaporation. The pH values were measured at the end of the experiment, and the water temperature of the beakers was 20.6 °C.

2.9. Statistical Analysis

The experimental ultimate tensile strength/tensile modulus, ultimate flexural strength/flexural modulus, and Charpy impact results for all formulations were compared individually using a one-way ANOVA F-test at a 95% confidence level since the variable changing was the filler quantity. The calculations were conducted with the Analysis ToolPak, a Microsoft Excel add-in program (Microsoft Corp., Redmond, WA, USA). If the F-critical value is less than the F-test value, the null hypothesis is rejected, indicating that the average was not the same for all groups. This suggests a statistically significant difference existed between the average values of each mechanical property for the different composite formulations. However, if the F-critical value approaches the F-test value, the null hypothesis cannot be rejected and considered as not being statistically significant.

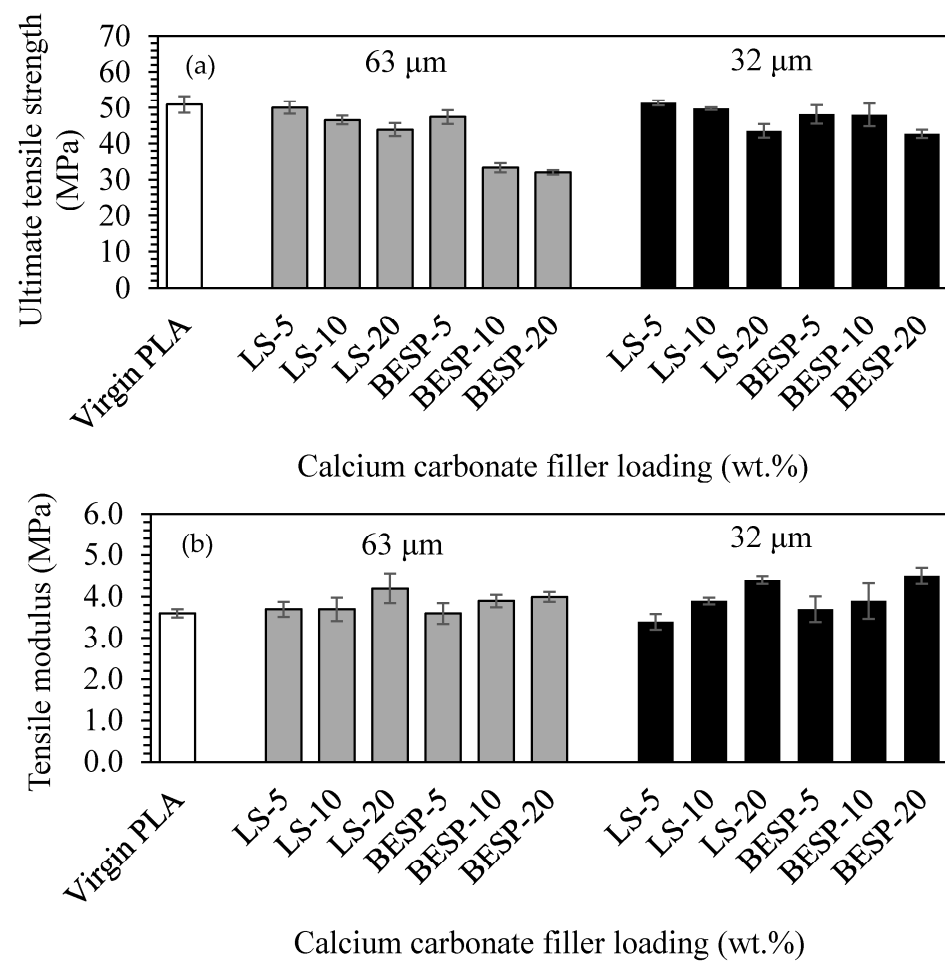
3. Results and Discussion

3.1. Mechanical Properties

The mechanical properties evaluated in this study are given in Table 2. The (±) symbols in Table 2 and the error bars in Figures 2–4 represent the standard deviations.

Table 2. Mechanical properties of PLA and PLA/calcium carbonate composite materials.

Composite	Ultimate Tensile Strength (MPa)	Tensile Modulus (GPa)	Ultimate Flexural Strength (MPa)	Flexural Modulus (GPa)	Charpy Impact Strength (kJm^{-2})
Virgin PLA	50.9 ± 2.3	3.6 ± 0.10	78.9 ± 4.2	2.9 ± 0.03	17.3 ± 0.70
Filler size ($63 \mu\text{m}$)					
LS-5	50.1 ± 1.8	3.7 ± 0.18	52.6 ± 5.0	3.1 ± 0.05	13.2 ± 0.90
LS-10	46.6 ± 1.2	3.7 ± 0.28	76.9 ± 5.4	3.2 ± 0.09	11.1 ± 1.5
LS-20	43.9 ± 1.8	4.2 ± 0.35	71.4 ± 2.7	3.4 ± 0.04	10.3 ± 1.0
BESP-5	47.4 ± 2.0	3.6 ± 0.25	46.5 ± 5.5	3.1 ± 0.04	8.7 ± 1.3
BESP-10	33.4 ± 1.3	3.9 ± 0.15	63.7 ± 7.6	3.1 ± 0.20	6.9 ± 0.70
BESP-20	32.1 ± 0.60	4.0 ± 0.12	21.5 ± 6.1	3.4 ± 0.11	6.5 ± 1.1
Filler size ($32 \mu\text{m}$)					
LS-5	51.3 ± 0.70	3.4 ± 0.19	67.2 ± 1.6	3.1 ± 0.03	14.8 ± 1.0
LS-10	49.8 ± 0.30	3.9 ± 0.08	92.7 ± 1.2	3.3 ± 0.03	14.0 ± 1.2
LS-20	43.5 ± 1.9	4.4 ± 0.09	91.0 ± 2.1	3.5 ± 0.05	11.2 ± 1.3
BESP-5	48.1 ± 2.6	3.7 ± 0.31	60.3 ± 1.1	3.1 ± 0.04	10.4 ± 1.1
BESP-10	48.0 ± 3.2	3.9 ± 0.43	66.8 ± 1.6	3.3 ± 0.10	7.8 ± 1.5
BESP-20	42.7 ± 1.2	4.5 ± 0.19	44.7 ± 1.5	3.4 ± 0.20	7.2 ± 1.4

**Figure 2.** Tensile properties of virgin PLA and PLA composites with calcium carbonate fillers: (a) ultimate tensile strength and (b) tensile modulus.

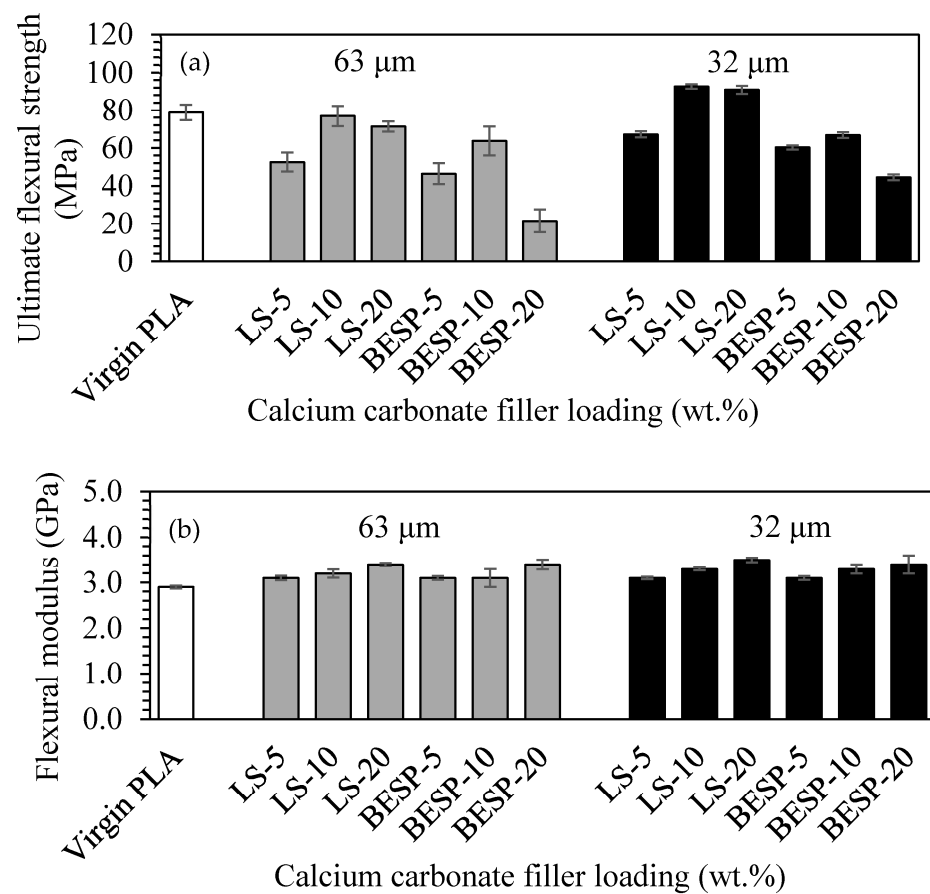


Figure 3. Flexural properties of virgin PLA and PLA composites with calcium carbonate fillers: (a) ultimate flexural strength and (b) flexural modulus.

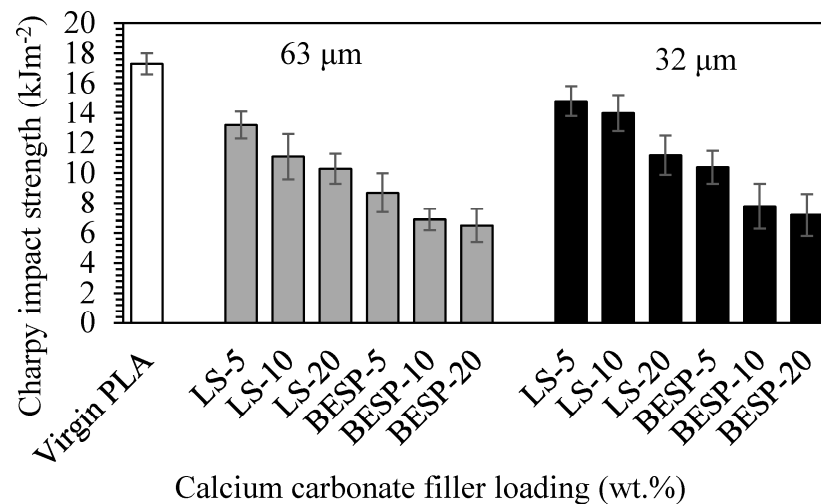


Figure 4. Charpy impact strength of virgin PLA and PLA composites with calcium carbonate fillers.

3.1.1. Tensile Properties

The tensile properties of the virgin PLA and PLA composites are summarized in Table 2 and shown in Figure 2 for two particle filler sizes (63 μm and 32 μm). The ultimate tensile strengths as a function of calcium carbonate filler loadings (Figure 2a) showed that composites containing 5 wt.% additions of LS and/or BEP for both particle sizes were similar to the control. When the loadings exceeded 5 wt.%, the strengths reduced below the control. This might be due to agglomeration of the fine filler powders in the PLA matrix,

which lack dispersion at higher loadings. At 10 wt.%, the ultimate tensile strengths for LS and BESP (63 μm) reduced by 8% and 34%, respectively, while LS and BESP (32 μm) decreased by 2% and 6%, respectively. Composites containing 5–10 wt.% BESP (32 μm) were similar in ultimate tensile strength. The conventional-limestone-filled composites were not substantially affected; however, the addition of the brown eggshell fillers to the PLA showed a sharper decrease in strength. At 20 wt.% concentrations, considerable reductions in ultimate tensile strengths were observed. In general, the smaller 32 μm particles performed slightly better than the larger 63 μm particles. The performances of PLA composites are partly dependent on the interaction of the matrix with the filler. At low filler loadings, it is probable there will be more polymer-filler-particle interactions and lower filler agglomerations. The presence of rigid limestone fillers tends to inhibit polymer chain motion during the uniaxial tensile test. When the filler content increases, the dispersion of the particles becomes non-uniform and the likelihood of filler particles clustering with each other increases (e.g., particle-to-particle interactions). In polymer composites, the agglomeration and poor adhesion between particles leads to lower tensile strengths [32]. In contrast to the tensile modulus, the tensile strength is susceptible to how well the bond forms between the filler/matrix interfaces since a poor link will interrupt the stress transfer from the matrix to the fillers [22]. Physical and chemical surface modifications have been applied to inorganic fillers to improve compatibility between synthetic polymers. A common physical treatment is the use of stearic acid, a fatty acid that acts as a surfactant. Stearic acid acts to lower the surface tension between the hydrophobic polymer and hydrophilic calcium carbonate particles by coating the particles with a hydrophobic film. A chemical treatment such as a coupling agent reacts with the surface of the calcium carbonate and the polymer matrix via chemical covalent bonding. Silane, titanate, and zirconate have been used as couplings agents [33].

The tensile modulus as a function of calcium carbonate filler loadings (Figure 2b) showed a steady increase as the filler content changed from 5 to 20 wt.%. Due to the higher stiffness of the filler particles, compared to the more-pliable PLA matrix, both the calcium carbonate filler types were rigid and will have less deformation when a tensile load is applied. As the filler loadings increase, the tendency and amount of particles interacting with the PLA polymer chains amplifies, resulting in less movement of the overall number of polymer chains and, thus, higher tensile moduli [34]. The differences in tensile modulus may be due to how well the fillers are dispersed during the manufacturing process. A study on the addition of halloysite, a clay mineral, as a filler to polypropylene showed a better dispersion of fillers, led to a greater tensile modulus [35]. In another study, Moreno et al. (2015) [36] investigated injection-molded calcium carbonate/PLA composites by blending them with a twin-screw extruder. The research revealed that increasing the screw speed resulted in a higher shear rate, which tended to improve the dispersion of the fillers in the PLA matrix.

3.1.2. Flexural Properties

The flexural properties of the virgin PLA and PLA composites are presented in Table 2 and Figure 3 for the two particle sizes studied. The ultimate flexural strengths as a function of calcium carbonate filler loadings (Figure 3a) showed that conventional limestone fillers produced better ultimate flexural strengths than brown eggshell fillers for all filler loadings. The ultimate flexural strengths of composites containing 10–20 wt.% LS for both particle sizes were on par with or higher than the virgin PLA. Composites containing 5–10 wt.% BESP (32 μm) had the highest ultimate flexural strengths when the sustainable eggshell fillers were used. Particle dimensions are an important characteristic of fillers that influences the reinforcement effect of the PLA biopolymer. Small-sized particles have a high surface area, which provides a large surface region for contact between the matrix and the particles [11]. However, small particles also tend to assemble into larger agglomerates due to electrostatic forces, and this increases with greater additions of filler loadings. This phenomenon can describe the drop in ultimate flexural strength at 20 wt.% loadings for all

composites. In contrast, large-sized particles do not agglomerate as much, but have a low surface area, which reduces the interaction between the matrix and filler when loads are applied to the composites. This factor is attributed to the lower strength of the composites containing 63 μm fillers compared to composites with 32 μm fillers.

The calcium carbonate fillers were able to provide a stiffening effect, as depicted by the flexural modulus results shown in Figure 3b. For both filler particle sizes, the flexural modulus increased with the increase of the filler content. At low loadings, the particles are anticipated to be well dispersed within the PLA matrix, resulting in larger inter-particle distances. As the filler content increases, the distances between the particles reduce, bringing particles closer to each other. This creates additional obstacles/restrictions for polymer chain mobility, which increase the flexural modulus. According to the results, it appears that the flexural modulus was less affected by the particle size and more by the amount of filler content.

3.1.3. Charpy Impact Properties

The Charpy impact strengths as a function of calcium carbonate filler loadings for the virgin PLA and PLA composites are provided in Table 2 and shown in Figure 4. The highest impact strength was observed for the virgin PLA. There was a gradual decrease of the impact strength with filler loading for all PLA composites; however, the composites with smaller particles sizes were slightly better. A study by Nakagawa and Sano (1985) [37] on polypropylene-filled calcium carbonate composites determined that smaller particles had better dispersion in the matrix and exhibited higher impact strengths. Toro et al. [38] studied the impact strength of polypropylene/eggshell composites. The authors noted that, although pure polypropylene samples experienced higher impact strengths, the addition of filler loadings reduced the total amount of polymer, which acted to decrease the toughness and impact strength of the composites. They also observed that composites with the highest tensile modulus (e.g., stiffness) exhibited the lowest impact properties due to the high stresses transferred from the polymer to the fillers. The impact strength could be affected by particle aggregation (e.g., particle-to-particle interactions), which leads to an inhomogeneous distribution of the fillers in the matrix. In addition, the forces holding particles together are adhesive forces such as weak secondary van der Waals forces. A study on the agglomeration tendency of eleven commercial calcium carbonate fillers was conducted ranging in particle sizes from 0.08 μm to 130 μm . The results indicated that the particle size was a controlling factor that determined the magnitude of the adhesive forces between particles where the aggregation of filler particles increased with decreasing particle size [39]. Although particle size is an important element, particle-to-particle aggregation has also been reported to be due to filler characteristics, specific surface area, composition, surface modification, surface tension, and process/manufacturing conditions [11,40].

The Charpy un-notched specimen test method measures the total energy needed for a crack to initiate and propagate. Un-notched testing can identify agglomeration in the composite material. Flaws in the form of large filler particles or large/small particles that agglomerate can be initiation points for cracks to generate and grow upon impact. Un-notched impact strengths obtained for polymers containing fillers has been reported to be sensitive to agglomerates [41]. In this study, the Charpy impact strengths decreased as the amounts of loadings increased, which suggests the un-notched samples were able to detect agglomerations in the polymer composite.

3.1.4. Scanning Electron Microscopy

Since the PLA composite's mechanical properties were generally better for the 32 μm fillers compared to the 63 μm fillers, SEM was conducted on the smaller particle sizes and fractured surfaces of composites containing these fillers. The particle microstructure for the powders of the conventional limestone (Figure 5a) and brown eggshells (Figure 5b) were similar in shape. The particles exhibited angular and irregular geometries for different sizes. The average particle size with the standard deviation (SD) for the 32 μm sieved

(No. 450 mesh) fillers was measured using the Image-J software (version 2.3.0/1.53f, NIH, Bethesda, Maryland, USA), where the LS and BE SP were $26.9 \pm 3.4 \mu\text{m}$ and $23.8 \pm 7.6 \mu\text{m}$, respectively, as shown in Figure 6.

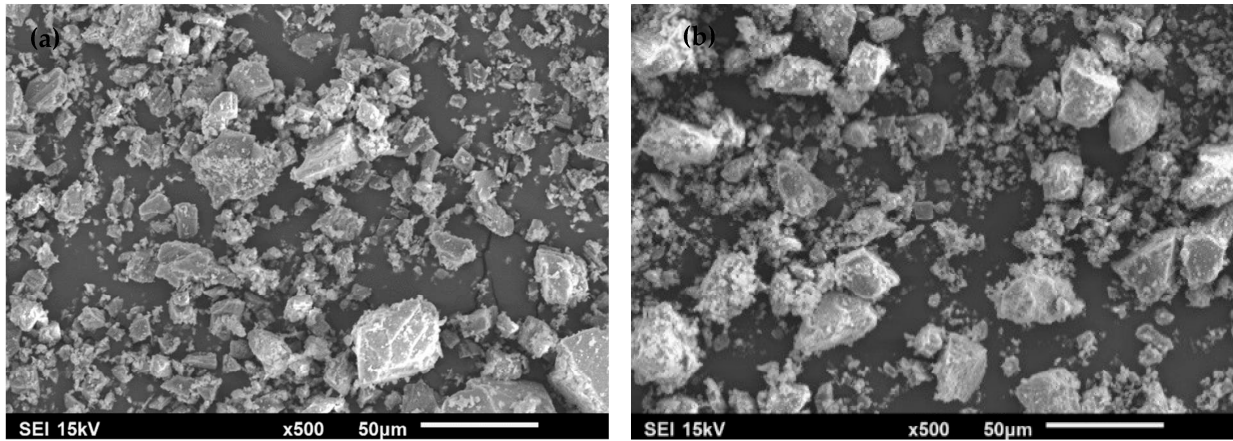


Figure 5. Scanning electron micrographs showing 32 μm powder morphologies: (a) conventional limestone and (b) brown eggshells.

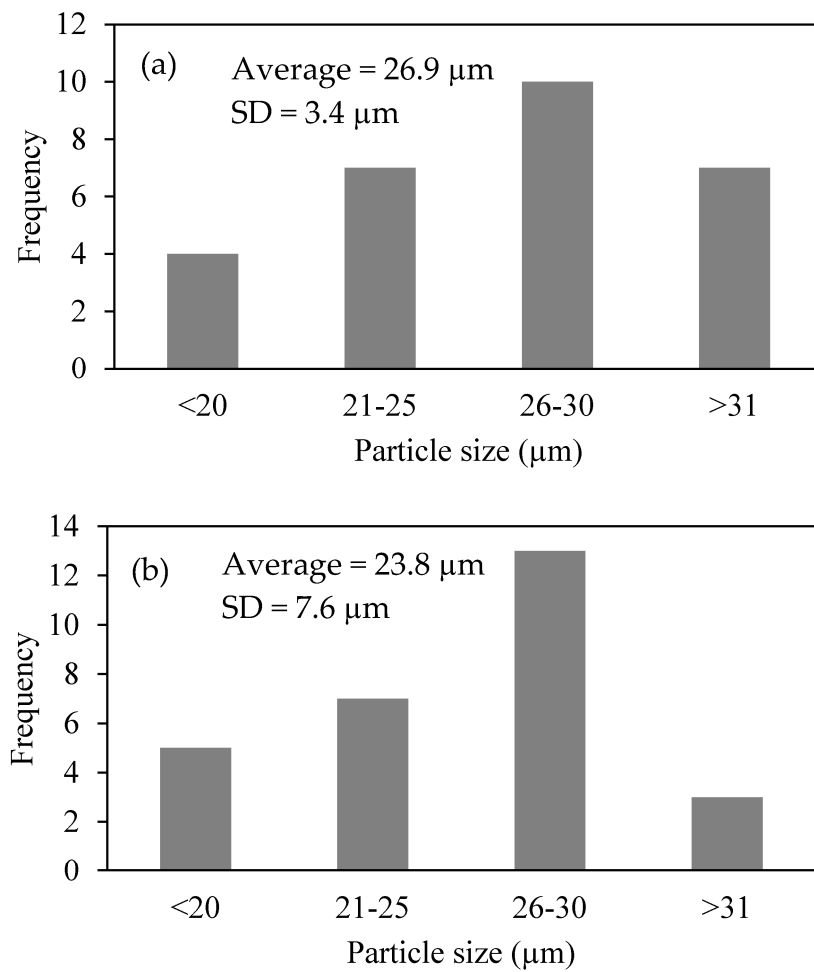


Figure 6. Size distribution of (a) conventional limestone and (b) brown eggshell fillers sieved to 32 μm .

The fractured surfaces of the tensile samples for the virgin PLA and the PLA composites containing the 32 μm sieved particles are shown in Figure 7. The morphology features of the virgin PLA (Figure 7a) were relatively smooth, revealing a brittle type of failure, which is characteristic of the PLA matrix. As the filler quantities increased, the surfaces were rougher, demonstrating ductile characteristics (Figure 7b–e), as given by the white ridges created during PLA stretching from the tensile test. From a visual observation, the virgin PLA (Figure 7a) and low filler content composites (Figure 7b,c) showed a dense fractured surface without any cavities, while at higher filler loadings (Figure 7d,e), some cavities were observed (red circles) due to pullout of the calcium carbonate fillers. This suggests the bonding between the filler and matrix was weak.

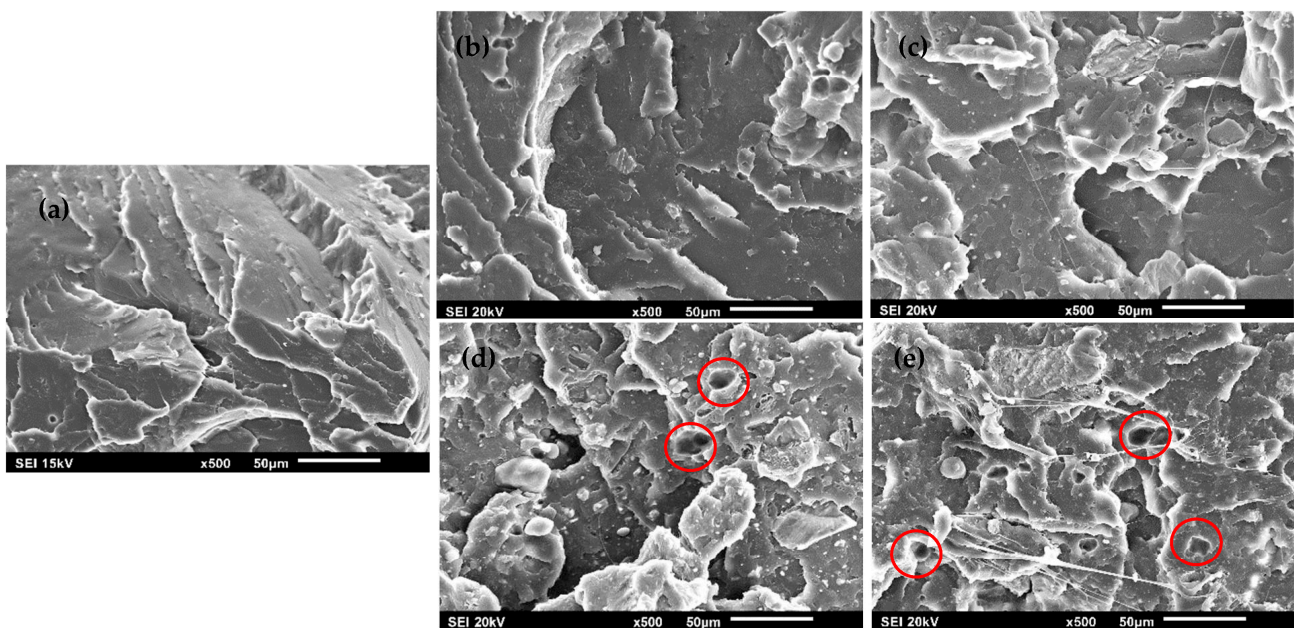


Figure 7. Scanning electron micrographs of tensile fractured surfaces: (a) virgin PLA, (b) PLA/LS-5, (c) PLA/BESP-5, (d) PLA/LS-20, and (e) PLA/BESP-20 (for 32 μm particles). Red circles show cavities in the matrix.

The SEM flexural fractured surfaces for the virgin PLA and the PLA composites containing 32 μm sieved particles are shown in Figure 8. Similar to the tensile fractured surfaces, the PLA without filler exhibited a brittle mode of failure, as depicted by the mostly flat regions in Figure 8a, while the filled PLA composites (Figure 8b–e) had irregular surfaces compared to the virgin PLA. When fillers were added (Figure 8b,c), the fractured surface after bending showed white fibrils, indicative of matrix plastic deformation. Void spaces were also concentrated around the stiff filler particles, as illustrated by the white regions, and this phenomenon was amplified at higher filler contents (Figure 8d,e). The particles appeared to be embedded in the fractured region of the PLA, suggesting synergy between the particles and matrix. However, during loading, the matrix deformed around the particles, indicating poor adhesion between the fillers and matrix.

The SEM Charpy impact fractured surfaces for the virgin PLA and PLA composites containing 32 μm particles are shown in Figure 9. The virgin PLA (Figure 9a) had flat areas associated with brittle fracture in addition to longitudinal patterns, which are linked to the crack propagation produced during impact loading. The PLA 5 wt.% composite fractured morphology (Figure 9b,c) appeared similar to the virgin PLA, which could explain the similar Charpy impact strength values associated with these materials, as echoed by the results in Figure 4. However, adding 20 wt.% loadings may be excessive, which caused embrittlement and reduced impact strength. By incorporating 20 wt.% fillers (Figure 9d,e), cavities appeared, possibly due to the dislodgement of filler particles in the matrix, as

highlighted by the red circles. At greater loadings, there was no specific direction to the crack propagation, and this can be observed from the irregular broken surfaces. This was also observed in a polypropylene/calcium carbonate composite, where the impact strength decreased as the fractured surface became rougher [42].

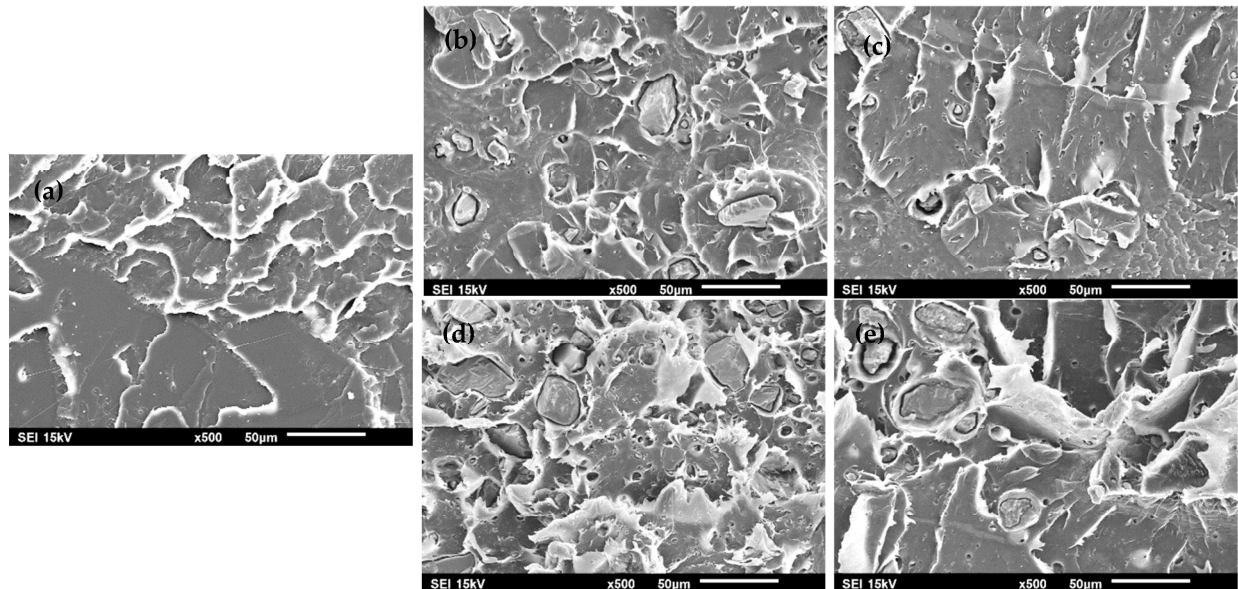


Figure 8. Scanning electron micrographs of flexural fractured surfaces: (a) virgin PLA, (b) PLA/LS-5, (c) PLA/BESP-5, (d) PLA/LS-20, and (e) PLA/BESP-20 (for 32 μm particles).

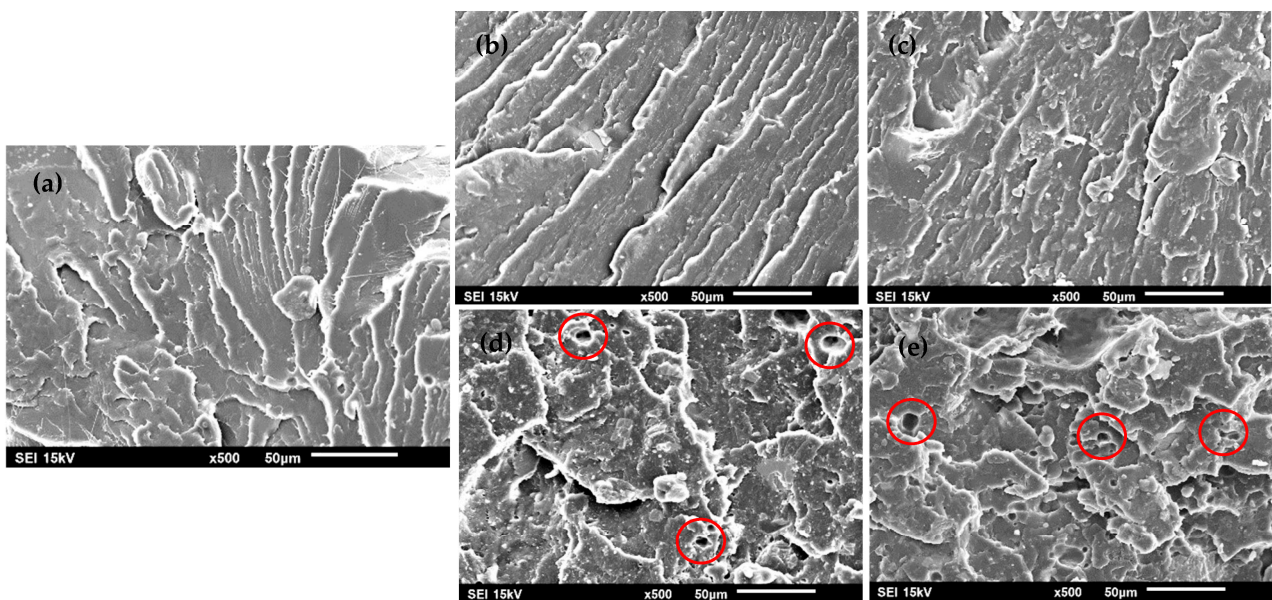


Figure 9. Scanning electron micrographs for Charpy impact fractured surfaces: (a) virgin PLA, (b) PLA/LS-5, (c) PLA/BESP-5, (d) PLA/LS-20, and (e) PLA/BESP-20 (for 32 μm particles). Red circles show cavities in the matrix.

3.1.5. Statistical Analysis

The tensile, flexural, and Charpy properties were assessed one-by-one for both particle sizes (63 μm and 32 μm), as given in Table 3. The mechanical property F-critical values were all less than the F-test values. Therefore, it can be concluded that a statistically significant difference existed between the average values of each property measured. The results of the

ANOVA analysis indicated that the addition of calcium carbonate filler materials (LS and BESP) to virgin PLA highly affected the tensile, flexural, and Charpy average properties.

Table 3. ANOVA mechanical property results of PLA containing calcium carbonate fillers (LS and BESP) with two different particle sizes of 63 μm and 32 μm .

Mechanical Property	Particle Size (μm)	Source of Variation	SS	df	MS	F-test	F-crit
Ultimate tensile strength (MPa)	63	BG	1431	6	238.6	84.49	2.508
		WG	67.77	24	2.824		
	32	BG	286.4	6	47.73	11.99	2.528
		WG	91.53	23	3.980		
Tensile modulus (GPa)	63	BG	1.527	6	0.2546	5.011	2.459
		WG	1.372	27	0.05080		
	32	BG	4.457	6	0.7429	12.54	2.490
		WG	1.482	25	0.0593		
Ultimate flexural strength (MPa)	63	BG	11,664	6	1944	72.61	2.549
		WG	589.0	22	26.77		
	32	BG	8255	6	1376	268.1	2.490
		WG	128.3	25	5.131		
Flexural modulus (GPa)	63	BG	0.9917	6	0.1653	42.92	2.549
		WG	0.0847	22	0.0039		
	32	BG	1.095	6	0.1825	21.42	2.490
		WG	0.2129	25	0.0085		
Charpy impact strength ($\text{KJ}\cdot\text{m}^{-2}$)	63	BG	858.6	6	143.1	129.4	2.246
		WG	69.68	63	1.106		
	32	BG	832.9	6	138.8	99.05	2.246
		WG	88.29	63	1.402		

BG, between groups; WG, within groups; SS, sum of squares; df, degree of freedom; MS, mean square.

3.1.6. Water Uptake

The water gains due to moisture content for the virgin PLA, as well as the PLA/LS and PLA/BESP composites containing 63 μm and 32 μm filler particles are shown in Figure 10. The water absorption weight gain for the virgin PLA at 2, 3, 4, and 5 weeks was 0.861%, 0.895%, 0.910%, and 0.910%, respectively. Similar results were obtained for an injection-molded PLA Ingeo Biopolymer 6100D polymer, where after 20 days (3 weeks) of immersion, the specimens reached their maximum capacity of about 1% of absorbed water [43]. The methyl side group of PLA provides hydrophobicity; however, PLA is not completely hydrophobic since water molecules are attracted to the polar oxygen linkages and end groups in the PLA molecule, which confers PLA's hydrophilicity [44]. The common consensus about PLA is that it is a polymer which attracts and absorbs moisture from the air over time. Following 5 weeks of water soaking, the composites containing LS and BESP particulates in amounts of 5, 10, and 20 wt.% had water weight gains of 0.910%, 0.983%, and 1.01% and 1.09%, 1.10%, and 1.13%, respectively for the 63 μm fillers. In the same way, composites containing 32 μm fillers had weight gains of 0.949%, 0.973%, and 1.09% and 1.10%, 1.15% and 1.26%, respectively. It was observed that smaller filler particle absorbed slightly more water than the larger 63 μm particles size. The physical absorption of water by fillers could be influenced by hydrophobicity/hydrophilicity, porosity, and surface area. Depending on the location of the sedimentary carbonate rock deposits, commercially available limestone can be of different purities. The majority of limestone contains calcium carbonate (CaCO_3) in the form of mineral calcite ranging in amounts of 85 wt.% (impure) to 98.5 wt.% (very high purity). The remaining are mineral impurities in the form of

lime (CaO), magnesia (MgO), silica (SiO₂), and iron oxide (Fe₂O₃) [45]. Correspondingly, brown eggshells have been determined to comprise calcium carbonate with calcite being the principal mineral [19]. For both mineral limestone and eggshells, the calcite material has a rhombohedral structure based on the hexagonal unit cell [46]. At the microscopic level, the eggshell contains two layers of calcite. The outermost layer (~5–8 μm thick) consists of dense vertical calcite crystals. The layer below is the palisade layer and is about 200 μm thick. It includes columnar calcite crystals that are less dense than the vertical layer and positioned perpendicular to the surface of the eggshell [47]. Calcite has been reported to be highly hydrophilic [48], where water interacts with the surface of calcite by electrostatic interaction and by hydrogen bonding [49]. Limestone as a rock and eggshell as a bio-ceramic structure both have high permeability. For example, depending on the limestone geological formation and depth of recovery, it can have porosities between 8% and 52% [50]. In the literature, the reported surface porosity for chicken eggshells as a percentage value (to compare against limestone) is limited; however, eggshells are porous as conveyed by the number of pores on the surface of the eggshell being between 10,000 and 20,000 [51]. The architecture of an eggshell is interesting such that the microscopic pore structure functions to permit oxygen to diffuse inwards through the shell from the surroundings and allows water vapor and carbon dioxide created by the chicken embryo to diffuse outwards [52]. In contrast to the larger filler particles (e.g., 63 μm), the water weight gain increased for composites containing smaller particles (e.g., 32 μm) since they tend to have a greater surface area suggesting more water contact with the particles.

As was anticipated, the composites incorporating 32 μm particles had for the most part better mechanical properties than composites containing the larger 63 μm particles. Therefore, the PLA mass loss samples, as well as calcium carbonate contents and pH levels of the distilled water mediums were evaluated for the former.

3.1.7. Mass Loss

After 5 weeks immersed in distilled water, the mass loss of the virgin PLA decreased by 0.102% as shown in Figure 11. The PLA/LS and PLA/BESP composites with 5, 10, and 20 wt.% loadings displayed mass losses of 0.120%, 0.127%, and 0.131% and 0.143%, 0.207%, and 0.235%, respectively. The mass losses were more observable for the brown eggshell composites. In the same way, a study immersed PLA (Ingeo 3051D) in water at 23 °C and 51 °C for 30 days and observed a minor weight decrease of 0.07% and 0.21%, respectively [53]. The degradation of PLA when submitted to high moisture or submerged in water can breakdown the matrix by a hydrolysis (e.g., reaction with water) mechanism, which results in a mass loss [54] and the lowering of its molecular weight [55]. At ambient temperature, the hydrolytic degradation of PLA is marginally stable to slow but is accelerated as the temperature of the water increases. A previous study illustrated that the time for PLA (structure type not mentioned) to degrade varied with temperature. For instance, temperatures of 4, 13, 25, 30, 50, 60, and 70 °C had onset fragmentation (e.g., ester groups of polylactide chains in the presence of water) times of 64 months, 25 months, 6 months, 4.4 months, 1.5 months, 8.5 days and 1.8 days, respectively [56].

Mass losses can be attributed to the hydrolysis of the matrix compounded with the hydrolysis of the matrix/filler interface. The PLA Ingeo 4043D used in the present study is a highly amorphous bio-polyester with a D-isomer content of 4.3%, providing its lower crystallinity [57]. PLA with less than 1% D-isomer is used in injection molding, where high crystallization rates are required, while higher contents (4–8%) reducing the crystallization rates, which can be advantageous for injection molding of optically transparent applications [58]. More importantly, amorphous thermoplastics are ideal over semi-crystalline polymers for injection molding since they have a lower-dimensional shrinkage with little to no crystallization, which acts to reduce warpage [59]. However, amorphous PLA structures are less stable against hydrolysis as the structure allows water to enter more easily into the bulk of the sample compared to a more-stable semi-crystalline PLA, as its structure prevents water diffusion into the bulk of the material [60]. Over time, water will break

down the high-molecular-weight PLA through hydrolysis. As the water molecules diffuse into the amorphous regions of the PLA, they react with ester bonds along the PLA backbone chain. This results in shorter, fragmented chains, which reduces the PLA's molecular weight. The hydrolysis process leads to ester bond cleavage occurring primarily in the amorphous regions, which produces water-soluble products such as lactic acid monomers and low-molecular-weight oligomer monomers. As time progresses, these products near the surface can leach out into the distilled water and PLA polymer degradation ensues [61]. Inorganic calcium carbonate is slightly soluble in pure water and has been reported to be between 6.8 mg/L [62] and 13 mg/L [63] at 25 °C. The solubility increases when the water contains carbon dioxide such as river water or rainwater found in nature. In addition, the solubility decreases with augmentation in temperature and increases with increasing mineral concentration [62]. As the composite absorbs water, the interface adhesion between the PLA matrix/industrial limestone and/or brown eggshell, fillers undergo hydraulic degradation, which promotes the detachment of filler particles [64]. It is hypothesized that the calcium-carbonate-based fillers are removed from the composite PLA surfaces as a solid material, which falls to the bottom of the beakers. A recent study attributed this phenomenon to osmosis degradation, where the calcium carbonate particles travel towards the external surfaces of the polymer composite and eventually are released into the aqueous media [65].

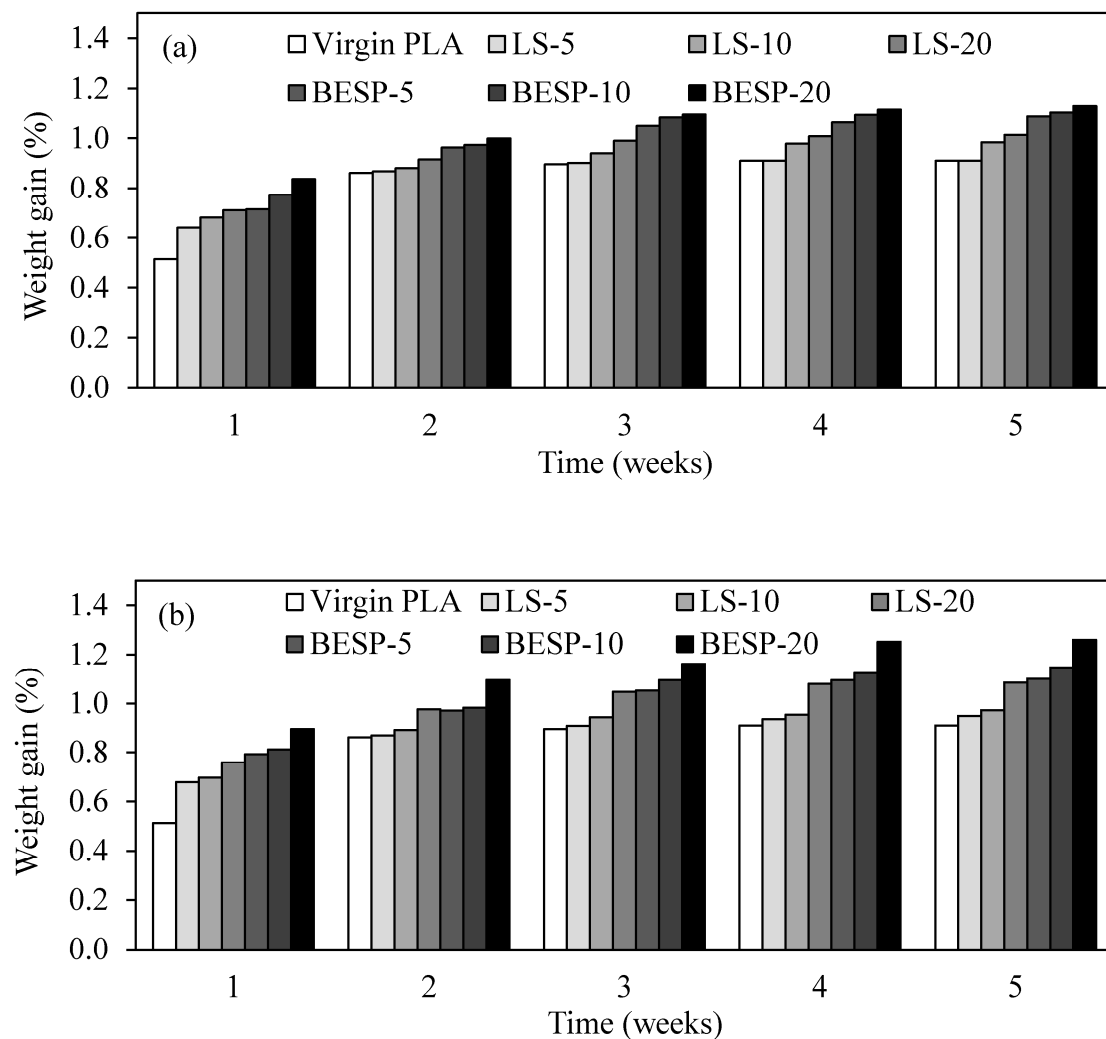


Figure 10. Weight gain due to moisture content for virgin PLA and PLA composites containing calcium carbonate fillers: (a) 63 µm particles and (b) 32 µm filler particles.

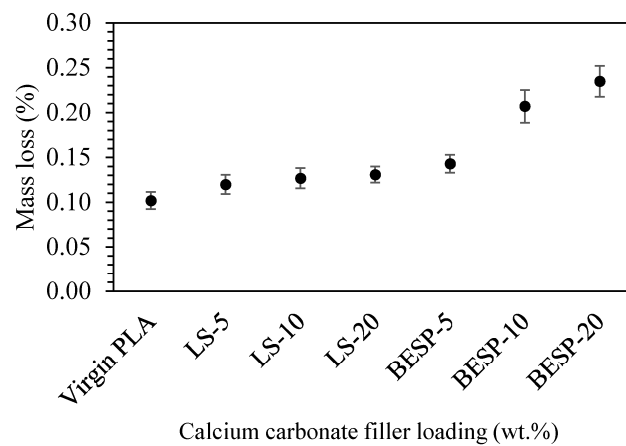


Figure 11. Mass loss after 5 weeks of the absorption test for virgin PLA and PLA composites containing 32 μm fillers at different loading concentrations.

3.1.8. Leaching Measurements

To determine the degree of leaching of the composites, if any, for both calcium-carbonate-based filler types (32 μm particles) and loadings, distilled water from individual beakers were tested after 5 weeks of water soaking, and the results are shown in Figure 12. An atomic absorption spectrophotometer was used to identify if calcium (Ca) was present in the water. The mass of calcium obtained was used to calculate the amount of CaCO_3 content in milligrams (mg) by multiplying the calcium content by a factor of 2.5. Distilled water and the virgin PLA water media were analyzed and did not contain any elemental calcium. Similarly, calcium traces in the PLA/LS composites were not detected. The PLA/BESP specimens with 5, 10 and 20 wt.% filler contents had 1.21, 2.05, and 4.68 mg of CaCO_3 , respectively. The results convey that the conventional limestone did not leach out of the PLA matrix in contrast to the brown eggshell particulates.

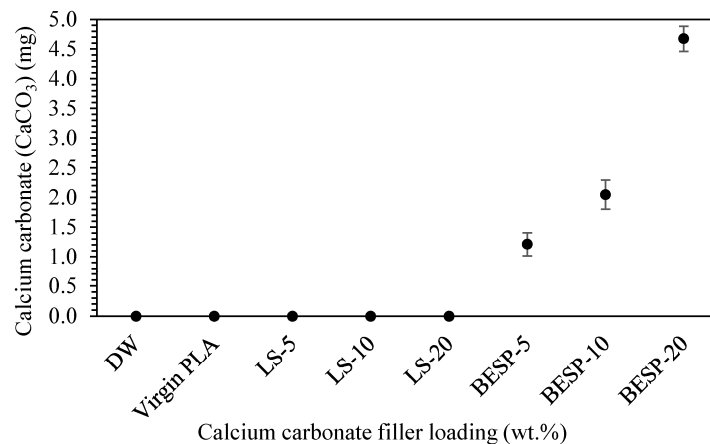


Figure 12. Calcium carbonate (CaCO_3) contents after 5 weeks in water for PLA composites containing 32 μm fillers at different loading concentrations.

Brown eggshells appeared to leach out more than mineral limestone, which can be due to the fact that there are amorphous regions of calcite within the crystalline calcite regions of the eggshell [66]. Amorphous regions are unstable and have a higher solubility in water than crystalline regions [67]. A “floating on water” test [68] was conducted where two beakers were filled with 100 mL of distilled water as shown in Figure 13a. Then, 5 g of the 32 μm -particle-size mineral limestone and brown eggshell powder were added in separate beakers (Figure 13b,c). The mixture was stirred at 1100 rpm for 5 min and allowed to settle for 5 days. From a visual observation, the majority of the mineral limestone beaded on top of the water, as depicted by the red arrow in Figure 13b, while a minor amount fell to the

bottom of the beaker. In contrast, all the eggshell powder settled to the bottom of the beaker. The eggshell powder mixed better with the distilled water than the mineral limestone possibly due to the attached membrane on the eggshells. The eggshell membrane consists of proteins that are hydrophilic, therefore, they absorb water and support the sinking of the eggshell particles to the bottom of the beaker. When high-comminution-degree limestone powders are stirred, cohesive interactions between small particles can be responsible for the pasting of grains [68]. The higher solubility of brown eggshells in water may be attributed to the greater leaching in the PLA/BESP composites.

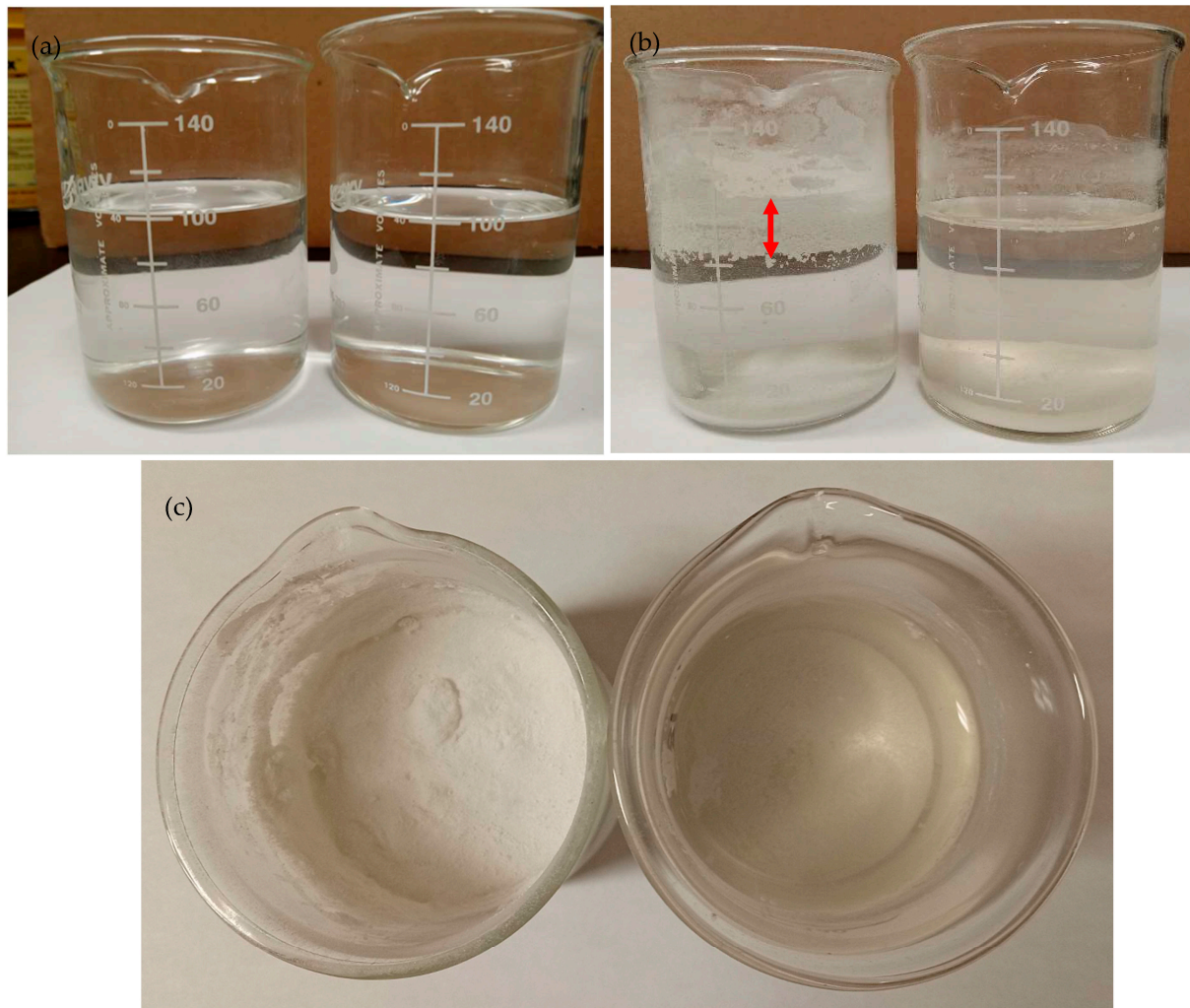


Figure 13. “Floating on water” test (a) prior to the addition of calcium carbonate, (b) side views after 5 days of rest for mineral limestone (left) and brown eggshells (right), and (c) top views after 5 days of rest for mineral limestone (left) and brown eggshells (right).

3.1.9. pH Measurements

Following the 5-week duration of water soaking, the leaching of PLA or calcium carbonate could cause the pH of the distilled water (DW) to change, as shown in Figure 14. As PLA breaks down in water, it creates an acidic medium due to carboxylic acid release [69]. In contrast, calcium carbonate offsets the acidic degradation products from PLA by increasing the pH [70]. The original distilled water had a measured pH of 6.17, and after the 5-week period, the pH value was 5.90. A reduction of the pH of the distilled water is indicative of the carbon dioxide (in the air) reaction with water to form carbonic acid. The virgin PLA water sample had a pH of 5.76, possibly due to marginal leaching of PLA. The PLA/LS and PLA/BESP composites had pH values of 5.83, 5.86, and

5.92 as well as 5.96, 6.05, and 6.33 for filler contents of 5, 10, and 20 wt.%, respectively. The PLA/LS composites had pH values in-line with the virgin PLA, while the pH values for the PLA/BESP composites rose slightly, which could be due to the leaching of the brown eggshell particles, as depicted in Figure 12.

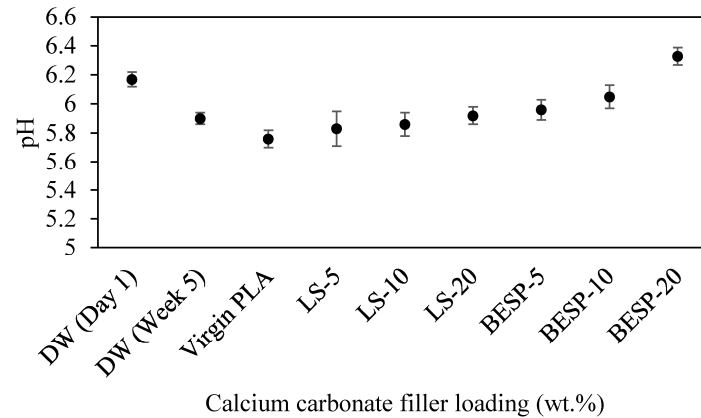


Figure 14. Variation of distilled water pH after 5 weeks for PLA composites containing 32 µm calcium carbonate fillers at different loading concentrations.

4. Conclusions

PLA composites containing either conventional limestone or brown eggshell fillers were prepared. For all mechanical properties, the additions of smaller particles were favored over larger particles, and conventional limestone performed marginally better than brown eggshells. The composites containing 5–10 wt.% brown eggshell fillers (32 µm) had the highest ultimate tensile strengths, while the additions of 10 wt.% brown eggshell fillers (32 µm) had the largest ultimate flexural strengths, but both properties were lower than the control. The tensile modulus and flexural modulus increased with filler loading; however, the Charpy impact strengths were lower than the control for both filler sizes of 63 µm and 32 µm. From scanning electron microscopy, changes in the fractured surfaces were observed from being relatively flat and smooth for virgin PLA to an increased roughness as the filler content increased. This suggests the additions of calcium carbonate fillers had the ability to alter the properties of the PLA. ANOVA showed that both filler size and filler contents had significant positive effects on the mechanical properties. The water uptake for the PLA/brown eggshell powder composites was greater than for the PLA/conventional limestone composites, which may be due to the porous architecture of the eggshell. Brown eggshell composites leached more than conventional limestone composites. The leaching was thought to be a result of the amorphous regions in the eggshells having a higher solubility than the conventional limestone. While the solubility of conventional limestone has been reported in the literature, there is a lack of solubility information for eggshells. The results indicated that waste brown eggshells are candidates for use as filler materials in polymer matrices.

Author Contributions: Conceptualization, D.C. and M.S.; methodology, D.C.; formal analysis, D.C., S.O. and M.S.; investigation, D.C.; resources, D.C.; data curation, D.C.; writing—original draft preparation, D.C.; writing—review and editing, D.C., S.O. and M.S.; supervision, D.C.; project administration, D.C.; funding acquisition, D.C. All authors have read and agreed to the published version of the manuscript.

Funding: The research was funded by the Natural Sciences and Engineering Research Council of Canada (NSERC) under the Discovery Grant (RGPIN-2020-06701). The APC was funded by MDPI.

Institutional Review Board Statement: Not applicable.

Informed Consent Statement: Not applicable.

Data Availability Statement: The data presented in this study are available upon request from the corresponding author. The data are not publicly available because the raw and processed data required to reproduce these findings cannot be shared at this time, as the data also form part of an ongoing study.

Acknowledgments: The authors would like to acknowledge Maple Lodge Hatcheries Ltd., Ontario, Canada, for the in-kind donation of the brown eggshells.

Conflicts of Interest: The authors declare no conflict of interest.

References

1. Al-Salem, S.M.; Lettieri, P.; Baeyens, J. Recycling and recovery routes of plastic solid waste (PSW): A review. *Waste Manag.* **2009**, *29*, 2625–2643. [CrossRef]
2. Geyer, R.; Jambeck, J.R.; Law, K.L. Production, use, and fate of all plastics ever made. *Sci. Adv.* **2017**, *3*, e1700782. [CrossRef]
3. Wright, S.L.; Thompson, R.C.; Galloway, T.S. The physical impacts of microplastics on marine organisms: A review. *Environ. Pollut.* **2013**, *178*, 483–492. [CrossRef] [PubMed]
4. Lebreton, L.; Slat, B.; Ferrari, F.; Sainte-Rose, B.; Aitken, J.; Marthouse, R.; Hajbane, S.; Cunsolo, S.; Schwarz, A.; Levivier, A.; et al. Evidence that the great pacific garbage patch is rapidly accumulating plastic. *Sci. Rep.* **2018**, *8*, 4666. [CrossRef]
5. Chamas, A.; Moon, H.; Zheng, J.; Qiu, Y.; Tabassum, T.; Jang, J.H.; Abu-Omar, M.; Scott, S.L.; Suh, S. Degradation rates of plastics in the environment. *ACS Sustain. Chem. Eng.* **2020**, *8*, 3494–3511. [CrossRef]
6. Market—European Bioplastics. 2022. Available online: <https://www.european-bioplastics.org/market/> (accessed on 20 July 2023).
7. Emadian, S.M.; Onay, T.T.; Demirel, B. Biodegradation of bioplastics in natural environments. *Waste Manag.* **2017**, *59*, 526–536. [CrossRef]
8. Chariyachotilert, C.; Joshi, S.; Selke, S.E.; Auras, R. Assessment of the properties of poly (L-lactic acid) sheets produced with differing amounts of postconsumer recycled poly (L-lactic acid). *J. Plast. Film Sheeting* **2012**, *28*, 314–335. [CrossRef]
9. Iñiguez-Franco, F.; Auras, R.; Dolan, K.; Selke, S.; Holmes, D.; Rubino, M.; Soto-Valdez, H. Chemical recycling of poly (lactic acid) by water-ethanol solutions. *Polym. Degrad. Stab.* **2018**, *149*, 28–38. [CrossRef]
10. Zuiderduin, W.C.J.; Westzaan, C.; Huetink, J.; Gaymans, R.J. Toughening of polypropylene with calcium carbonate particles. *Polymer* **2003**, *44*, 261–275. [CrossRef]
11. Leong, Y.W.; Abu Bakar, M.B.; Ishak, Z.M.; Ariffin, A.; Pukanszky, B. Comparison of the mechanical properties and interfacial interactions between talc, kaolin, and calcium carbonate filled polypropylene composites. *J. Appl. Polym. Sci.* **2004**, *91*, 3315–3326. [CrossRef]
12. McNeill, I.C.; Mohammed, M.H. Thermal analysis and degradation mechanisms of blends of low density polyethylene, poly(ethyl acrylate) and ethylene ethyl acrylate copolymer with calcium carbonate. *Polym. Degrad. Stab.* **1995**, *49*, 263–273. [CrossRef]
13. Osman, M.A.; Atallah, A.; Suter, U.W. Influence of excessive filler coating on the tensile properties of LDPE–calcium carbonate composites. *Polymer* **2004**, *45*, 1177–1183. [CrossRef]
14. Wang, W.Y.; Zeng, X.F.; Wang, G.Q.; Chen, J.F. Preparation and characterization of calcium carbonate/low-density-polyethylene nanocomposites. *J. Appl. Polym. Sci.* **2007**, *106*, 1932–1938. [CrossRef]
15. Mantia, F.P.L.; Morreale, M.; Scaffaro, R.; Tulone, S. Rheological and mechanical behavior of LDPE/calcium carbonate nanocomposites and microcomposites. *J. Appl. Polym. Sci.* **2013**, *127*, 2544–2552. [CrossRef]
16. Bomal, Y.; Godard, P. Melt viscosity of calcium-carbonate-filled low density polyethylene: Influence of matrix-filler and particle-particle interactions. *Polym. Eng. Sci.* **1996**, *36*, 237–243. [CrossRef]
17. Teixeira, S.C.S.; Moreira, M.M.; Lima, A.P.; Santos, L.S.; Da Rocha, B.M.; De Lima, E.S.; da Costa, R.A.; da Silva, A.L.N.; Rocha, M.C.; Coutinho, F.M. Composites of high density polyethylene and different grades of calcium carbonate: Mechanical, rheological, thermal, and morphological properties. *J. Appl. Polym. Sci.* **2006**, *101*, 2559–2564. [CrossRef]
18. Cree, D.; Rutter, A. Sustainable bio-inspired limestone eggshell powder for potential industrialized applications. *ACS Sustain. Chem. Eng.* **2015**, *3*, 941–949. [CrossRef]
19. Pliya, P.; Cree, D. Limestone derived eggshell powder as a replacement in Portland cement mortar. *Constr. Build. Mater.* **2015**, *95*, 1–9. [CrossRef]
20. Toro, P.; Quijada, R.; Yazdani-Pedram, M.; Arias, J.L. Eggshell, a new bio-filler for polypropylene composites. *Mater. Lett.* **2007**, *61*, 4347–4350. [CrossRef]
21. Lin, Z.; Zhang, Z.; Mai, K. Preparation and properties of eggshell/ β -polypropylene bio-composites. *J. Appl. Polym. Sci.* **2012**, *125*, 61–66. [CrossRef]
22. Ghabeer, T.; Dweiri, R.; Al-Khateeb, S. Thermal and mechanical characterization of polypropylene/eggshell biocomposites. *J. Reinf. Plast. Compos.* **2013**, *32*, 402–409. [CrossRef]
23. Feng, Y.; Ashok, B.; Madhukar, K.; Zhang, J.; Zhang, J.; Reddy, K.O.; Rajulu, A.V. Preparation and characterization of polypropylene carbonate bio-filler (eggshell powder) composite films. *Int. J. Polym. Anal. Charact.* **2014**, *19*, 637–647. [CrossRef]
24. Kumar, R.; Dhaliwal, J.S.; Kapur, G.S.; Shashikant. Mechanical properties of modified biofiller-polypropylene composites. *Polym. Compos.* **2014**, *35*, 708–714. [CrossRef]

25. Shuhadah, S.; Supri, A.G. LDPE-isophthalic acid modified egg shell powder composites (LDPE/ESPI). *J. Phys. Sci.* **2009**, *20*, 87–98.
26. Sivarao; Salleh, M.R.; Kamely, A.; Tajul, A.; Taufik, R.S. Mechanical properties modification of polyethylene (PE) for CaCO₃ particulated composites. *Adv. Mater. Res.* **2011**, *264*, 880–887.
27. Nwanonyeni, S.C.; Obidiegwu, M.U.; Onuchukwu, T.S.; Egbuna, I.C. Studies on the properties of linear low density polyethylene filled oyster shell powder. *Int. J. Eng. Sci.* **2013**, *2*, 42.
28. Hassan, S.B.; Aigbodion, V.S.; Patrick, S.N. Development of polyester/eggshell particulate composites. *Tribol. Ind.* **2012**, *34*, 217.
29. Hassan, T.A.; Rangari, V.K.; Jeelani, S. Value-added biopolymer nanocomposites from waste eggshell-based CaCO₃ nanoparticles as fillers. *ACS Sustain. Chem. Eng.* **2014**, *2*, 706–717. [[CrossRef](#)]
30. Ashok, B.; Naresh, S.; Reddy, K.O.; Madhukar, K.; Cai, J.; Zhang, L.; Rajulu, A.V. Tensile and thermal properties of poly (lactic acid)/eggshell powder composite films. *Int. J. Polym. Anal. Charact.* **2014**, *19*, 245–255. [[CrossRef](#)]
31. Cree, D.; Soleimani, M. Bio-Based White Eggshell as a Value-Added Filler in Poly (Lactic Acid) Composites. *J. Compos. Sci.* **2023**, *7*, 278. [[CrossRef](#)]
32. Liang, J.Z. Toughening and reinforcing in rigid inorganic particulate filled poly (propylene): A review. *J. Appl. Polym. Sci.* **2002**, *83*, 1547–1555. [[CrossRef](#)]
33. Rong, M.Z.; Zhang, M.Q.; Ruan, W.H. Surface modification of nanoscale fillers for improving properties of polymer nanocomposites: A review. *Mater. Sci. Technol.* **2006**, *22*, 787–796. [[CrossRef](#)]
34. Tan, M.A.; Yeoh, C.K.; Teh, P.L.; Rahim, N.A.A.; Song, C.C.; Voon, C.H. Effect of zinc oxide suspension on the overall filler content of the PLA/ZnO composites and cPLA/ZnO composites. *e-Polymers* **2023**, *23*, 20228113. [[CrossRef](#)]
35. Wei, T.; Jin, K.; Torkelson, J.M. Isolating the effect of polymer-grafted nanoparticle interactions with matrix polymer from dispersion on composite property enhancement: The example of polypropylene/halloysite nanocomposites. *Polymer* **2019**, *176*, 38–50. [[CrossRef](#)]
36. Moreno, J.F.; da Silva, A.L.N.; da Silva, A.H.M.D.F.T.; de Sousa, A.M.F. Preparation and characterization of composites based on poly (lactic acid) and CaCO₃ nanofiller. In *AIP Conference Proceedings*; AIP Publishing: Melville, NY, USA, 2015; Volume 1664. [[CrossRef](#)]
37. Nakagawa, H.; Sano, H. *Improvement of Impact Resistance of Calcium Carbonate Filled Polypropylene and Poly-Ethylene Block Copolymer*; Polymer Preprints, Division of Polymer Chemistry; American Chemical Society: Chicago, IL, USA, 1985; pp. 249–250.
38. Toro, P.; Quijada, R.; Arias, J.L.; Yazdani-Pedram, M. Mechanical and morphological studies of poly (propylene)-filled eggshell composites. *Macromol. Mater. Eng.* **2007**, *292*, 1027–1034. [[CrossRef](#)]
39. Pukánszky, B.; Fekete, E. Aggregation tendency of particulate fillers: Determination and consequences. *Polym. Polym. Compos.* **1998**, *6*, 313–322.
40. Lazzeri, A.; Thio, Y.S.; Cohen, R.E. Volume strain measurements on CaCO₃/polypropylene particulate composites: The effect of particle size. *J. Appl. Polym. Sci.* **2004**, *91*, 925–935. [[CrossRef](#)]
41. DeArmitt, C. Understanding filler interactions improves impact resistance. *Plast. Addit. Compd.* **2006**, *8*, 34–39. [[CrossRef](#)]
42. Zhu, Y.D.; Allen, G.C.; Jones, P.G.; Adams, J.M.; Gittins, D.I.; Heard, P.J.; Skuse, D.R. Dispersion characterisation of CaCO₃ particles in PP/CaCO₃ composites. *Compos. Part A Appl. Sci. Manuf.* **2014**, *60*, 38–43. [[CrossRef](#)]
43. Eselini, N.; Tirkes, S.; Akar, A.O.; Tayfun, U. Production and characterization of poly (lactic acid)-based biocomposites filled with basalt fiber and flax fiber hybrid. *J. Elastomers Plast.* **2020**, *52*, 701–716. [[CrossRef](#)]
44. Dugan, J.S. Novel properties of PLA fibers. *Int. Nonwoovens J.* **2001**, *3*, 1558925001OS-01000308.
45. Mitchell, C. High purity limestone quest. *Ind. Miner.* **2011**, *531*, 48–51.
46. Alamillo-López, V.M.; Sánchez-Mendieta, V.; Olea-Mejía, O.F.; González-Pedroza, M.G.; Morales-Luckie, R.A. Efficient removal of heavy metals from aqueous solutions using a bionanocomposite of eggshell/Ag-Fe. *Catalysts* **2020**, *10*, 727. [[CrossRef](#)]
47. Hincke, M.T.; Nys, Y.; Gautron, J.; Mann, K.; Rodriguez-Navarro, A.B.; McKee, M.D. The eggshell: Structure, composition and mineralization. *Front. Biosci.-Landmark* **2012**, *17*, 1266–1280. [[CrossRef](#)]
48. Walker, R.A.; Wilson, K.; Lee, A.F.; Woodford, J.; Grassian, V.H.; Baltrusaitis, J.; Rubasinghege, G.; Cibir, G.; Dent, A. Preservation of York Minster historic limestone by hydrophobic surface coatings. *Sci. Rep.* **2012**, *2*, 880. [[CrossRef](#)]
49. Hakim, S.S.; Olsson, M.H.M.; Sørensen, H.O.; Bovet, N.; Bohr, J.; Feidenhans'l, R.; Stipp, S.L.S. Interactions of the calcite {10.4} surface with organic compounds: Structure and behaviour at mineral–organic interfaces. *Sci. Rep.* **2017**, *7*, 7592. [[CrossRef](#)] [[PubMed](#)]
50. Cassar, J. *Deterioration of the Globigerina Limestone of the Maltese Islands*; Special Publications; Geological Society: London, UK, 2002; Volume 205, pp. 33–49.
51. Baxter-Jones, C. Egg hygiene: Microbial contamination, significance and control. In *Avian Incubation, Proceedings of the Poultry Science Symposium, West of Scotland College, Auchincruive, Ayr, Scotland, 12–15 September 1989*; No. 22; Tullett, S.G., Ed.; Butterworth: London, UK, 1991; pp. 269–276.
52. Mueller, C.A.; Burggren, W.W.; Tazawa, H. The physiology of the avian embryo. In *Sturkie's Avian Physiology*; Academic Press: Cambridge, MA, USA, 2022; pp. 1015–1046.
53. Ndazi, B.S.; Karlsson, S. Characterization of hydrolytic degradation of polylactic acid/rice hulls composites in water at different temperatures. *Express Polym. Lett.* **2011**, *5*, 119–131. [[CrossRef](#)]

54. Casalini, T.; Rossi, F.; Castrovinci, A.; Perale, G. A perspective on polylactic acid-based polymers use for nanoparticles synthesis and applications. *Front. Bioeng. Biotechnol.* **2019**, *7*, 259. [[CrossRef](#)] [[PubMed](#)]
55. Taib, R.M.; Ramarad, S.; Ishak, Z.A.M.; Todo, M. Properties of kenaf fiber/polylactic acid biocomposites plasticized with polyethylene glycol. *Polym. Compos.* **2010**, *31*, 1213–1222. [[CrossRef](#)]
56. Lunt, J. Large-scale production, properties and commercial applications of polylactic acid polymers. *Polym. Degrad. Stab.* **1998**, *59*, 145–152. [[CrossRef](#)]
57. Ortenzi, M.A.; Gazzotti, S.; Marcos, B.; Antenucci, S.; Camazzola, S.; Piergiovanni, L.; Farina, H.; Di Silvestro, G.; Verotta, L. Synthesis of polylactic acid initiated through biobased antioxidants: Towards intrinsically active food packaging. *Polymers* **2020**, *12*, 1183. [[CrossRef](#)]
58. Wang, Y.; Xu, Y.; He, D.; Yao, W.; Liu, C.; Shen, C. “Nucleation density reduction” effect of biodegradable cellulose acetate butyrate on the crystallization of poly (lactic acid). *Mater. Lett.* **2014**, *128*, 85–88. [[CrossRef](#)]
59. Oliaei, E.; Heidari, B.S.; Davachi, S.M.; Bahrami, M.; Davoodi, S.; Hejazi, I.; Seyfi, J. Warp and shrinkage optimization of injection-molded plastic spoon parts for biodegradable polymers using Taguchi, ANOVA and artificial neural network methods. *J. Mater. Sci. Technol.* **2016**, *32*, 710–720. [[CrossRef](#)]
60. Fukushima, K.; Feijoo, J.L.; Yang, M.C. Comparison of abiotic and biotic degradation of PDLA, PCL and partially miscible PDLA/PCL blend. *Eur. Polym. J.* **2013**, *49*, 706–717. [[CrossRef](#)]
61. Limsukon, W.; Auras, R.; Selke, S. Hydrolytic degradation and lifetime prediction of poly (lactic acid) modified with a multifunctional epoxy-based chain extender. *Polym. Test.* **2019**, *80*, 106108. [[CrossRef](#)]
62. Larson, T.E.; Sollo, F.W., Jr.; McGurk, F.F. Complexes affecting the solubility of calcium carbonate in water. In *ISWS Contract Report CR 145*; University of Illinois at Urbana-Champaign Water Resources Center: Urbana, IL, USA, 1973.
63. Tegethoff, F.W.; Rohleder, J.; Kroker, E. (Eds.) *Calcium Carbonate: From the Cretaceous Period into the 21st Century*; Springer Science & Business Media: Berlin/Heidelberg, Germany, 2001.
64. Tamboura, S.; Abdessalem, A.; Fitoussi, J.; Daly, H.B.; Tcharkhtchi, A. On the mechanical properties and damage mechanisms of short fibers reinforced composite submitted to hydrothermal aging: Application to sheet molding compound composite. *Eng. Fail. Anal.* **2022**, *131*, 105806. [[CrossRef](#)]
65. Abdessalem, A.; Tamboura, S.; Fitoussi, J.; Ben Daly, H.; Tcharkhtchi, A. Bi-phasic water diffusion in sheet molding compound composite. *J. Appl. Polym. Sci.* **2020**, *137*, 48381. [[CrossRef](#)]
66. Li, Y.; Li, Y.; Liu, S.; Tang, Y.; Mo, B.; Liao, H. New zonal structure and transition of the membrane to mammillae in the eggshell of chicken *Gallus domesticus*. *J. Struct. Biol.* **2018**, *203*, 162–169. [[CrossRef](#)]
67. Kendall, J. XCVI. The solubility of calcium carbonate in water. *Lond. Edinb. Dublin Philos. Mag. J. Sci.* **1912**, *23*, 958–976. [[CrossRef](#)]
68. Vogt, E. Effects of Commercial modifiers on flow properties of hydrophobized limestone powders. *Pol. J. Environ. Stud.* **2013**, *22*, 1213–1218.
69. Sabir, M.I.; Xu, X.; Li, L. A review on biodegradable polymeric materials for bone tissue engineering applications. *J. Mater. Sci.* **2009**, *44*, 5713–5724. [[CrossRef](#)]
70. Al-Shirawi, M.; Karimi, M.; Al-Maamari, R.S. Impact of carbonate surface mineralogy on wettability alteration using stearic acid. *J. Pet. Sci. Eng.* **2021**, *203*, 108674. [[CrossRef](#)]

Disclaimer/Publisher’s Note: The statements, opinions and data contained in all publications are solely those of the individual author(s) and contributor(s) and not of MDPI and/or the editor(s). MDPI and/or the editor(s) disclaim responsibility for any injury to people or property resulting from any ideas, methods, instructions or products referred to in the content.